Geophysical Research Letters

RESEARCH LETTER
10.1029/2019GL086903

QBO Changes in CMIP6 Climate Projections

Neal Butchart[1], James A. Anstey[2], Yoshio Kawatani[3], Scott M. Osprey[4,5], Jadwiga H. Richter[6], and Tongwen Wu[7]

[1]Met Office Hadley Centre, Exeter, UK, [2]Canadian Centre for Climate Modelling and Analysis, Victoria, British Columbia, Canada, [3]Japan Agency for Marine-Earth Science and Technology, Yokohama, Japan, [4]National Centre for Atmospheric Science, University of Oxford, Oxford, UK, [5]Department of Physics, University of Oxford, Oxford, UK, [6]Climate and Global Atmosphere Division, National Center of Atmospheric Research, Boudler, CO, USA, [7]Beijing Climate Center, China Meteorological Administration, Beijing, China

Abstract Phase 6 of the Coupled-Model Intercomparison Project (CMIP6) is the first in which a significant number of models include a well-resolved stratosphere. Changes in equatorial stratospheric variability in historical and Shared Socioeconomic Pathways (SSPs) scenario simulations are investigated in 10 models with realistic quasi-biennial oscillations (QBO). All project a weakening of the QBO throughout the stratosphere for SSP370 and SSP585 scenarios and for 1960 to 2010. The weakening is strongest in the lower stratosphere, ranging from 5.8 ± 0.5% to 4.3 ± 0.5 % to 2.0 ± 0.5% per decade at 50 hPa for SSP585, SSP370, and historical simulations, respectively. At 20 hPa a weakening of both westward and eastward phases contributes though the weakening eastward phase is only seen in 7 of the 10 models. Similar robust weakening occurs for the temperature QBO, but only from 30 hPa upward. In both scenarios the QBO period decreases in 7 of the 10 models.

Plain Language Summary At altitudes between roughly 16 and 50 km the equatorial atmosphere is dominated by strong zonal winds that reverse sign from eastward to westward roughly every 14 months in what is referred to as the quasi-biennial oscillation. With developments in models the quasi-biennial oscillation now features in a significant number of the latest state-of-the-art climate projections. In those projections featuring the oscillation, the changing climate weakens it by up to ~6% per decade for the more extreme of the scenarios considered. Somewhat less certain is a shortening of the time between wind reversals in several of the projections.

Key Points:
- Many more CMIP6 models simulate a QBO than in previous CMIP phases
- A weakening of the QBO in response to climate change is projected by 10 CMIP6 models with realistic QBOs
- Under warming scenarios QBO periods shorten in 7 of the 10 CMIP6 models with realistic QBOs

Correspondence to:
N. Butchart,
neal.butchart@metoffice.gov.uk

Citation:
Butchart, N., Anstey, J. A., Kawatani, Y., Osprey, S. M., Richter, J. H., & Wu, T. (2020). QBO changes in CMIP6 climate projections. *Geophysical Research Letters*, *47*, e2019GL086903. https://doi.org/10.1029/2019GL086903

Received 31 DEC 2019
Accepted 12 FEB 2020
Accepted article online 18 FEB 2020

1. Introduction

The quasi-biennial oscillation (QBO) is arguably the most distinctive internal mode of natural variability seen anywhere in the Earth's atmosphere. It consists of alternate layers of eastward and westward winds that descend through the equatorial stratosphere from roughly 50 km down to ~16 km (Baldwin et al., 2001). Periods range from 21 to 32 months, averaging around 28 months, and the oscillation is generally symmetric about the equator with a meridional half width of about 12° (Baldwin et al., 2001). In reanalyses, amplitudes at the equator peak at around 30 m/s at 20 hPa (Coy et al., 2016). Surface climate is influenced by the oscillation through teleconnections to the troposphere either directly (e.g., Hendon & Abhik, 2018) or via the polar stratosphere (e.g., Andrews et al., 2019; Anstey & Shepherd, 2014). Changes in the teleconnections therefore have the potential to alter tropospheric circulations patterns and, in turn, are likely to depend on changes to the QBO.

Prior to Phase 6 of the Coupled Model Intercomparison Project (CMIP6; Eyring et al., 2016), very few of the models providing the projections used for the Intergovernmental Panel on Climate Change (IPCC) assessments (e.g., IPCC, 2013) were capable of simulating a QBO. Partially, this was due to poorly resolved stratospheres in many of the earlier models. Five models featured a QBO for CMIP5 (Butchart et al., 2018; Schenzinger et al., 2017) and from an analysis of four of these models Kawatani and Hamilton (2013) were the first to report the possibility that climate change weakens the QBO. This possibility was confirmed by Richter, Butchart, et al. (2020) with an analysis of 11 models that performed identical idealized 1 × CO_2, 2 × CO_2, and 4 × CO_2 time-slice simulations for Phase 1 of the Stratospheric-tropospheric Processes And their Role in Climate QBO-initiative (QBOi; Butchart et al., 2018), though the atmosphere-only models used

were often not as comprehensive as those used for state-of-the-art climate projections. Both Kawatani and Hamilton (2013) and Richter, Butchart, et al. (2020) noted that there was no consensus among the models on how the QBO period would respond to a changing climate.

A generally under appreciated development introduced with the CMIP6 multimodel ensemble is the increased number of models representing stratospheric processes, with 15 out 30 models now able to simulate realistic QBO-like behavior in the equatorial stratosphere during the historical period (Richter, Anstey, et al., 2020a). The CMIP6 simulations therefore provide a new opportunity to quantify, with increased confidence, QBO changes seen in state-of-the-art climate projections. However, several of the model runs' diagnostics required for analyzing the mechanisms driving the QBO changes are not currently available in the CMIP6 international archive. Thus, the aim here is to focus on quantifying changes in the simulated zonal wind and temperature QBO to provide the necessary and timely input for building a comprehensive picture of circulation changes in the latest CMIP6 climate projections underpinning the upcoming IPCC assessment (Eyring et al., 2016). An investigation of the drivers of the QBO changes is left for a follow-up study, while the overall fidelity of the simulated QBOs in CMIP6 models is discussed in Richter, Anstey, et al. (2020a).

2. Data and Models

Monthly mean data from 10 CMIP6 models that completed the historical and Shared Socioeconomic Pathways (SSPs, Gidden et al., 2019) 370 and 585 scenario simulations (Eyring et al., 2016; O'Neill et al., 2016) are used here. ScenarioMIP (O'Neill et al., 2016) provided concentrations of all long-lived greenhouse gases (CO_2, CH_4, N_2O, and CFCs) for two high-end scenarios that achieve climate forcings of 7.0 and 8.5 W/m^2 by 2100, and the corresponding CO_2 concentrations (Meinshausen et al., 2019) in 2100 in the SSP370 and SSP585 simulations are 867 and 1,135 parts per million (ppm), respectively. All 10 models simulated broadly realistic QBOs (Richter, Anstey, et al., 2020a). Five other models also exhibit realistic QBOs in the historical period (Richter, Anstey, et al., 2020a), but output for one or both of the scenario simulations is not currently available in the CMIP6 international archive. For each simulation, data are used from all realizations labeled r1, r2, r3, and r4 that are currently available in the central archive (i.e., ensembles of up to four members are used).

Data from the following models (Insitutes) are used: BCC-CSM2-MR (BCC) [3,1,1], CESM2-WACCM (NCAR) [3,1,1], CNRM-CM6-1 (CNRM-CERFAX) [4,4,4], CNRM-ESM2-1 (CNRM-CERFAX) [4,4,4], EC-Earth3 (EC-Earth-Consortium) [2,2,2], EC-Earth3-Veg (EC-Earth-Consortium) [4,3,3], IPSL-CM6A-LR (IPSL) [4,4,4], MIROC6 (MIROC) [4,3,3], MRI-ESM2-0 (MRI) [4,4,1], and UKESM1-0-LL (MOHC) [4,4,4], with the number of historical, SSP370, and SSP585 ensemble members used, respectively, given in the square brackets. The models are more comprehensive than the QBOi models used by Richter, Butchart, et al. (2020) with coupled oceans and in some cases additional Earth system components. On the other hand, QBOi models were specifically tuned for simulating the QBO (Butchart et al., 2018). Both groups of models have well-resolved stratospheres, and, on average, differences between the two groups in representing historical QBO amplitudes are small (Richter, Anstey, et al., 2020a).

Three-dimensional monthly-mean zonal-wind and temperature data on the standard CMIP6 pressure levels (1,000, 925, 850, 700, 600, 500, 400, 300, 250, 200, 150, 100, 70, 50, 30, 20, 10, 5, and 1 hPa) were obtained from the CMIP6 database (Balaji et al., 2018) for 1850–2014 for the historical simulation and 2015–2100 for the SSP370 and SSP585 scenario simulations. Zonal means of these data are then averaged over the latitude band 5° S to 5° N. As in Kawatani and Hamilton (2013), the resultant time series are smoothed with a five month running mean. Multimodel mean trends for QBO amplitudes and periods are calculated after first calculating the mean trend for each model by averaging the trends obtained for each ensemble member (realization).

3. Results

3.1. Amplitudes

Figure 1 shows the time series of the equatorially averaged (5° S to 5° N) monthly and zonal mean eastward winds at 20 hPa for single realizations of the SSP585 scenario simulations. Results for the other realizations analyzed are broadly similar. Despite a wide spread in detail, all the models display QBO-like behavior with the winds alternating from westward to eastward quasiperiodically. A similar signal is seen at 30 hPa

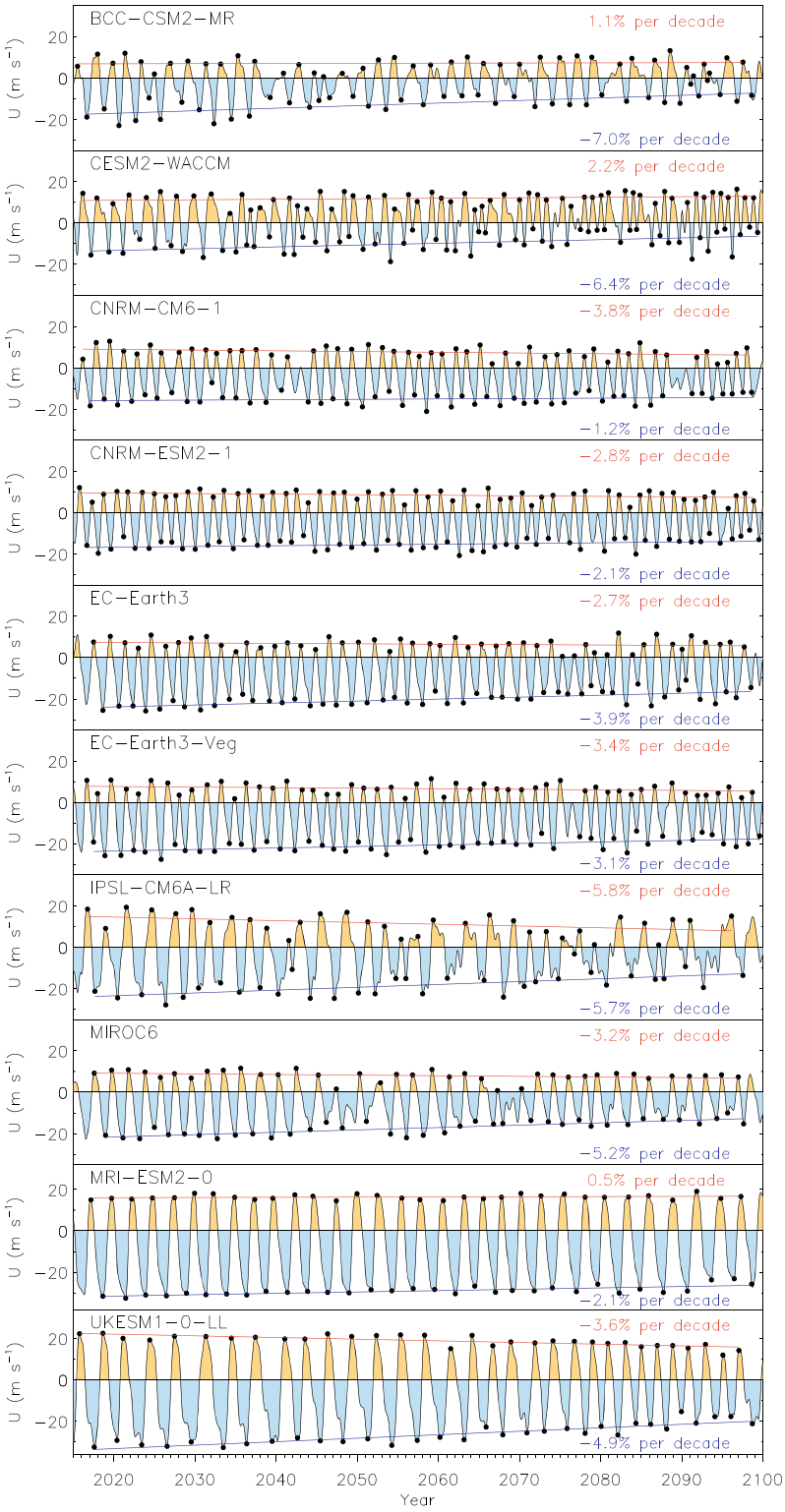

Figure 1. For SSP585 scenario simulations (Realization r1): 5-month running-mean zonal and monthly mean eastward wind averaged 5° S to 5° N at 20 hPa. Black dots indicate the eastward and westward maximum of each QBO cycle defined by the transitions from westward to eastward winds. Single month and transitions implying very short periods (≤9 months) are excluded. In the panels cycles can be identified by noting that each contains one consecutive pair of eastward and westward maxima. Red and blue lines denote least squares fits to the eastward and westward maxima, respectively. Negative values for the slope (specified in % per decade in each panel) indicate decreasing amplitude for that phase.

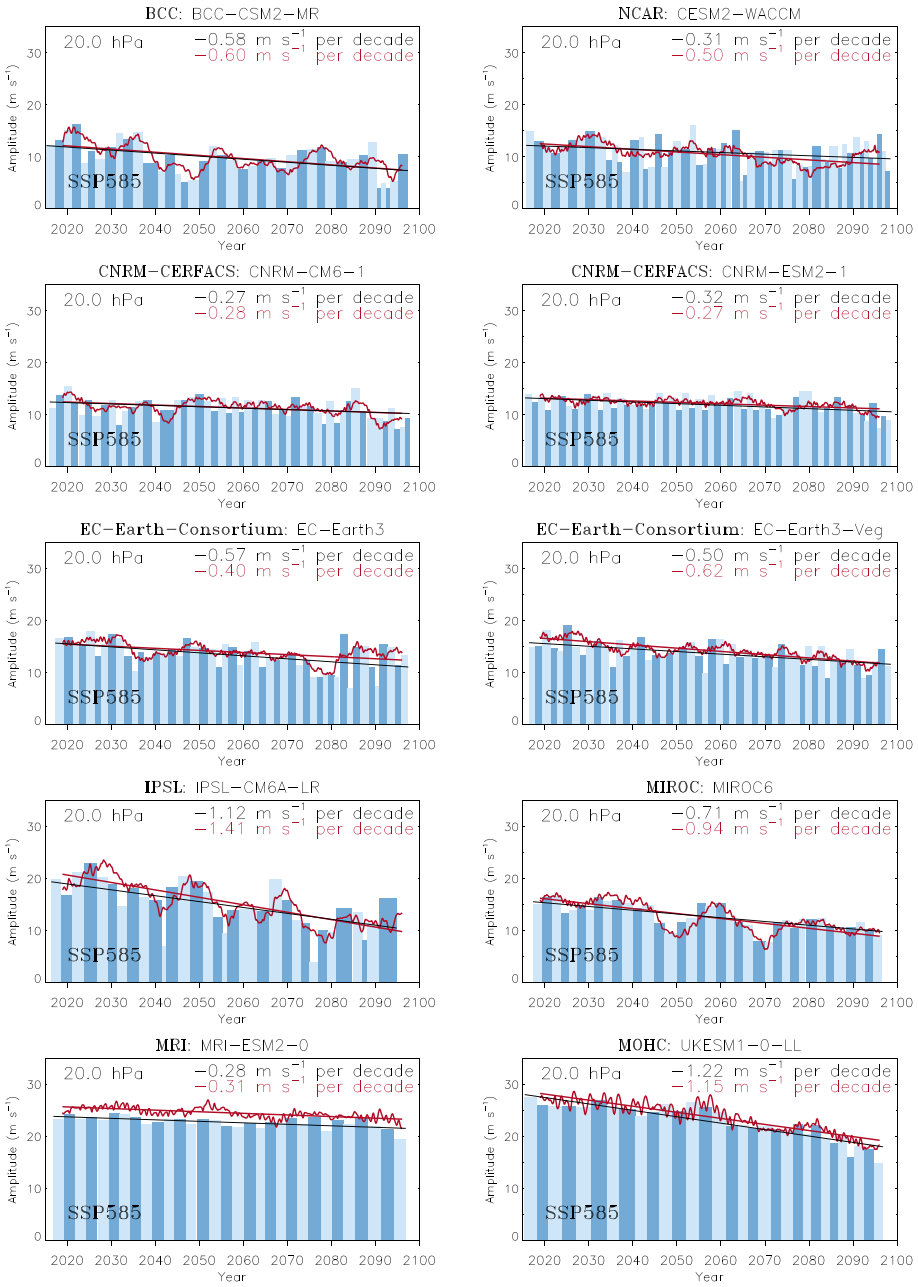

Figure 2. Bar graphs showing for Realization r1 of the SSP585 scenario simulations the amplitude (half the sum of consecutive eastward and westward maxima shown in Figure 1) of each QBO cycle at 20 hPa. Light and dark shading is used to help distinguish the individual cycles with the width of each bar denoting the period of that cycle. The black lines are the linear trends in amplitude assuming the time for each amplitude point is the start of each cycle. The red lines are estimated amplitudes calculated after the removal of the mean seasonal cycle as the $\sqrt{2}\times$root mean squares for a moving 8-year time window (see text for details) together with the corresponding least squares linear fit. The points on the red curve represent the midpoint of the moving 8-year window.

(not shown) confirming that the characteristic downward phase propagation associated with the QBO is present. However, at other stratospheric levels (70, 50, and 10 hPa) distinct QBO cycles are not always clearly discernible in all the models, particularly toward the end of the century. This breakdown of a coherent QBO signal toward the end of SSP585 scenario simulations is consistent with the findings of Richter, Butchart, et al. (2020) for 4×CO_2 time-slice simulations. Even at 20 hPa in the CMIP6 simulations uncertainty can arise when identifying individual cycles for some models as can be seen, for instance, with the CESM2-WACCM simulation (Figure 1). Nonetheless, this uncertainty is not considered critical for the conclusion of this paper,

as alternative diagnostics are also used to quantify the QBO's amplitude response to a changing climate (see below). During the historical simulations, the regular quasiperiodic behavior is more clearly discernible for all the models considered here (see Richter, Anstey, et al., 2020a).

Based on the peak eastward and westward winds in each QBO cycle (as defined in Figure 1) under the SSP585 scenario, all models project a weakening of the westward phase at an average rate of 4.16% per decade (blue lines in Figure 1). The weakening of the eastward phase is not quite so robust with three models (BCC-CSM2-MR, CESM2-WACCM, and MRI-ESM2-0) projecting a modest strengthening (red lines in Figure 1). On average, the amplitude of the eastward phase decreases at a rate of 2.15% per decade—about half the rate of decrease projected for the westward phase. The average of consecutive eastward and westward maxima (i.e., half the peak-to-peak value) provides a measure of the QBO amplitude for that cycle, and these are shown by the bar graphs in Figure 2 (periods are also given by the widths of the bars—see below). A downward trend (black lines) in amplitudes is robust across all 10 models and ranges from −0.27 m/s per decade for CNRM-CM6-1 to −1.22 m/s per decade for UKESM1-0-LL. Along with this weakening of the QBO there is also a slight narrowing in latitude (not shown) of the oscillation in all the models, at least at 20 hPa.

As in Kawatani and Hamilton (2013) QBO amplitudes are also estimated using a methodology first proposed by Dunkerton and Delisi (1985) who argued that the root mean square of the deseasonalized time series multiplied by the square root of 2 provides a good estimate of the QBO's amplitude when it is the dominant mode of variability. Kawatani and Hamilton (2013) adapted this approach and estimated amplitudes for overlapping periods of three cycles duration. Instead of periods of three cycles, overlapping 8-year periods are used here (i.e., amplitudes are calculated for a moving 8-year window). The use of a fixed number of years instead of cycles avoids the complications associated with identifying QBO cycles based on transitions from westward to eastward winds. Tests using the same observational data as Kawatani and Hamilton (2013) showed that amplitudes estimated either using the three-cycle window or 6-, 8-, 10-, or 12-year windows are broadly similar. Therefore, the 8-year window is chosen, as it is similar in length to the three-cycle window used by Kawatani and Hamilton (2013) and eliminates the uncertainties associated with the need to identify QBO cycles.

The red lines in Figure 2 are the estimated amplitudes (root mean squares multiplied by the square root of 2) based on an 8-year moving window, advanced in monthly increments. Bushell et al. (2020) showed that mean QBO amplitudes estimated using the Dunkerton and Delisi (1985) method agreed well with those obtained by identifying individual QBO cycles. The results shown in Figure 2 extend this and show that by using a moving window, it is possible to capture both variability and secular trends in amplitude. On average the trend for the estimated amplitudes is −0.65 m/s per decade compared to −0.59 m/s per decade for amplitudes based on identifying distinct QBO cycles. A corollary to this agreement is the implication that uncertainty associated with identifying individual cycles is unlikely to be critical, at least for the results reported here. In general, the largest differences between the two methods for calculating amplitudes occurs in those models in which the variability in amplitude is greatest (e.g., CESM2-WACCM, EC-Earth3, EC-Earth3-Veg, IPSL-CM6A-LR, and MIROC6). In turn, the BCC-CSM2-MR results show that large variability in amplitude is not always associated with differences in the trends estimated in the two different ways.

3.2. Periods

From the widths of the bars in Figure 2, it is clear that a wide spread exists in the periods of individual QBO cycles irrespective of secular changes resulting from the SSP585 climate forcings. The underlying spread in periods among models is considered further in Richter, Anstey, et al. (2020a) for the historical simulations. Here the focus is on the secular changes in period, and corresponding linear trends are tabulated in Table 1 for the SSP370 and SSP585 scenarios, along with the mean periods and intercycle standard deviation for each model. Occasionally, in Figure 2 cycles occur that appear anomalously long for a particular model (e.g., EC-Earth3-Veg in the late 2070s) though a closer inspection of Figure 1 usually indicates that this is due to the uncertainties noted above in clearly identifying the QBO cycle transitions and, arguably, the "long-cycle" should instead be treated as two shorter cycles. Likewise, there are times when it can be argued that two consecutive short cycles are actually a single cycle with longer period. However, tests showed that splitting the long cycles or combining short cycles when there is uncertainty in identifying cycle transitions is unlikely to have any significant impact on the analysis of the trends presented here.

Table 1
QBO Periods for SSP370 and SSP585 Scenario Simulations

	SSP370		SSP585	
	Mean ± std	Trend	Mean ± std	Trend
BCC-CSM2-MR	24.9 ± 5.3	−0.11(−2.1)	24.9 ± 5.8	−0.06(−1.1)
CESM2-WACCM	20.0 ± 5.4	**−0.17(−4.2)**	17.2 ± 5.5	**−0.17(−5.4)**
CNRM-CM6-1	19.6 ± 3.7	−0.05(−1.4)	19.7 ± 5.0	−0.05(−1.4)
CNRM-ESM2-1	17.8 ± 3.9	−0.01(−0.4)	17.5 ± 3.5	−0.05(−0.9)
EC-Earth3	19.7 ± 3.2	−0.02(−0.6)	19.6 ± 3.4	**−0.08(−2.2)**
EC-Earth3-Veg	20.6 ± 4.0	0.02(−0.6)	20.6 ± 4.7	0.01(0.3)
IPSL-CM6A-LR	30.5 ± 8.7	0.13(1.6)	30.6 ± 9.1	0.04(0.3)
MIROC6	25.0 ± 4.8	−0.06(−1.1)	25.9 ± 4.7	−0.05(−0.8)
MRI-ESM2-0	31.4 ± 2.3	0.06(0.7)	31.3 ± 2.4	0.9(1.2)
UKESM1-0-LL	33.0 ± 6.2	**−0.38(−3.5)**	30.5 ± 6.4	**−0.45(−4.6)**
Multimodel mean[†]	24.3 ± 3.7	(−1.1 ± 1.2)	23.8 ± 3.7	(−1.5 ± 1.4)

Note. Mean periods and intercycle standard deviation (std) are expressed in months and for each model are calculated for the distribution of cycles from all ensemble members used. Trends are the average of the trends from the individual ensemble members and are expressed in months per cycle. The number in brackets after the trends is the equivalent trend in % per decade. Trends are shown bold when the average statistical significance (calculated using a lag-1 autocorrelation to account for the nonindependence of the residual values about the trend line as described in section 4 of Santer et al., 2008) for the ensemble used is more than 95%.
[†]The multimodel mean is the mean of the mean period or trend (in % per decade) from the individual models with the uncertainty (i.e., 2 standard error) given after the ± sign.

Seven out of the 10 models project a decrease in the period of the QBO for the SSP585 scenario (Table 1) at an average rate of 2.3% per decade (cf. 1.5% per decade average for all 10 models). However, the decrease is only statistically significant, on average, at the 95% confidence level in three of the models (CESM2-WACCM, EC-Earth3, and UKESM1-0-LL). Nonetheless, results for the SSP370 scenario simulations (Table 1) lend support to the reliability of the projected decrease in the seven models, though the negative trends are now only statistically significant in CESM2-WACCM and UKESM1-0-LL. For the seven models projecting a shorter period in both scenarios, the mean rates of decrease are 1.9% and 2.3% per decade for the SSP370 and SSP585 scenarios, respectively, which is consistent with the stronger climate forcing in the SSP585 scenario. The highest rate of increase in the length of the QBO period is 1.6% per decade in the IPSL-CM6A-LR model for the SSP370 scenario, falling to a lengthening of 0.3% per decade for the SSP585 scenario. Therefore, even in this model, there is some evidence that with strong climate forcing, there is the possibility of the oscillation speeding up compared to when the forcing is weaker (i.e., the SSP370 scenario).

Also listed in Table 1 are the mean periods and cycle-to-cycle variability or standard deviation. For each model neither the mean nor the standard deviation differ much between scenarios. Likewise, the multimodel mean periods for the SSP370 and SSP585 scenarios are similar at 24.3 and 23.8 months, respectively. In both scenarios the uncertainty (2 standard error) in the multimodel mean is comparable to the cycle-to-cycle variability (standard deviation) in the individual models. Differences in cycle-to-cycle variability between the models do not appear related to the differences in mean periods. On the other hand, across all the models the variability is large, and hence, the detection of small trends in the periods is problematic. Trends themselves may also be underestimated due to the models not fully accounting for climate change in their parameterization of gravity waves.

3.3. Multimodel Mean Projections

3.3.1. QBO Amplitudes—Winds

Based on the good agreement at 20 hPa between QBO amplitudes calculated from half the peak eastward to peak westward amplitude for each cycle and amplitudes estimated from the root mean squares multiplied by the square root of 2, and their concomitant trends (see Figure 2 for SSP585 simulations), amplitudes are estimated using the latter method for all stratospheric levels, including those where the individual QBO cycles where not always clearly discernible, and linear trends calculated. Profiles of the multimodel mean

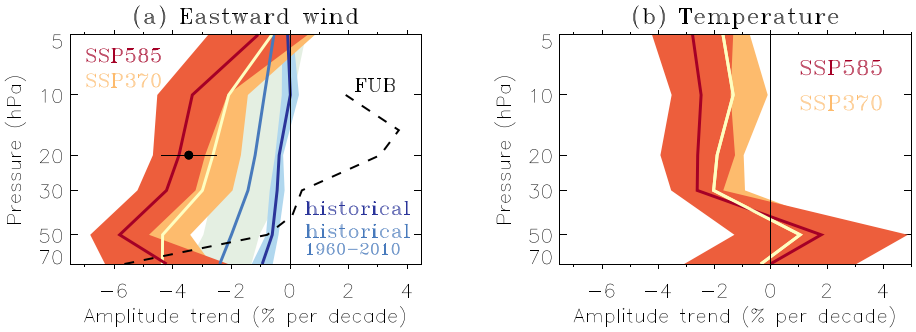

Figure 3. Multimodel mean trend (% per decade) in QBO amplitudes for SSP370 and SSP585 scenarios as a function of height for (a) eastward wind and (b) temperatures. Amplitudes are calculated from the root mean squares of the deseasonalized time series multiplied by the square root of 2 for an 8-year moving window (see text for details). For the temperatures the time series are first detrended by subtracting the least squares linear fit. Shading denotes the uncertainty in the multimodel mean (±2 standard error). In (a) trends are also shown for the whole historical simulation (1850–2014) and for the 50 years 1960–2010 to allow a comparison with observations (dashed black line). The dashed black line in (a) is the trend calculated for the observations for 1960–2010 obtained from the Freie Universität of Berlin (at https://www.geo.fu-berlin.de/en/met/ag/strat/produkte/qbo). The black dot in (a) is the multimodel mean trend and its uncertainty (2 standard error) for the SSP585 scenario calculated from half the peak eastward to peak westward amplitudes of the individual QBO cycles shown in Figure 1

trend are shown in Figure 3a for the historical and SSP370 and SSP585 scenario simulations. Trends for the historical run are shown for the full period (1850–2014) and the 50 years 1960–2010. Shading denotes the intermodel spread (±2 standard error). The little black dot represents the multimodel mean trend and its uncertainty (2 standard error) calculated from half the peak-to-peak amplitudes for the SSP585 simulations shown in Figures 1 and 2 and confirms the good agreement between the two approaches for deducing trends.

Between 70 and 10 hPa amplitudes decrease, on average, in all simulations with the majority of the decrease in the historical period coming from the most recent 50 years 1960–2010 (2.0% per decade compared to 0.6% per decade for the full historical period). Over the period 1960–2010 the rate of decrease in amplitude declines from 2.4% per decade at 70 hPa to 0.6% per decade at 5 hPa. For both scenarios trends also weaken with height through the stratosphere, except for the SSP585 scenario for which amplitudes decrease most rapidly at 50 hPa rather than 70 hPa. Possibly, the falling off in the trend below 50 hPa in the SSP585 simulations is due to an overall upward displacement of the QBO similar to that seen in the $4 \times CO_2$ experiments analyzed by Richter, Butchart, et al. (2020). Trends at 50 hPa are 2.0 ± 0.5, 4.3 ± 0.5, and 5.8 ± 0.5% per decade for 1960–2010 and the SSP370 and SSP585 scenarios, respectively. At this level the CMIP6 multimodel trend for 1960–2010 agrees reasonably well with the trend (black dashed line in Figure 3) calculated for the observed monthly mean winds obtained from the Freie Universität of Berlin (FUB; Naujokat, 1986). However, at other levels the agreement is not good with the FUB data indicating a strengthening of the amplitude above 30 hPa and a very strong negative trend at the lowest level (70 hPa). Possible reasons for these discrepancies are discussed in Kawatani and Hamilton (2013), who note that the reliability of 50-year trends at the higher levels from a single realization such as FUB data is questionable due to variability in trends.

3.3.2. QBO Amplitudes—Temperatures

A QBO signal has been known to exist in equatorial stratospheric temperatures for almost as long as the signal in the winds (e.g., Ebdon & Veryard, 1961). To analyze how this signal changes in the CMIP6 projections, the background cooling of the stratosphere due to climate change is first removed from the time series of monthly mean temperatures by subtracting out the linear trend. Temperature amplitudes for the QBO are then calculated from the time series of residual anomalies in the same way as the amplitudes for the winds are calculated using the root mean squares multiplied by the square root of 2 for an 8-year moving window (see above). Results are shown in Figure 3b for the two scenario simulations.

In contrast to the winds that showed the largest percentage weakening of the QBO at the lowest two levels (70 and 50 hPa), there is no corresponding robust decrease in the estimated temperature amplitudes at these levels (Figure 3). On average, the temperature amplitudes increase at 50 hPa although, because of the large intermodel spread, some models actually project a decrease in the temperature amplitude at this level. From 30 hPa upward all models project a weakening of the temperature QBO for both scenarios. As expected, the

weakening is, on average, more pronounced for the SSP585 scenario. At these levels the mean trends in the temperature amplitudes are slightly smaller in % per decade than those in the wind amplitudes, as are the differences between the two scenarios (cf. Figures 3a and 3b). Also, at these levels the trends in Figure 3b are roughly constant in altitude unlike those for the zonal wind (Figure 3a), which, due to thermal wind balance, is more closely related to the second derivative of temperature across the equator than temperature itself (e.g., section 8.2 in Andrews et al., 1987).

4. Discussion and Conclusions

The period of the QBO is essentially determined by its descent rate through the stratosphere (Baldwin et al., 2001). Opposing the descent is tropical upwelling due to the Brewer-Dobson circulation (Dunkerton, 1997). A speeding-up of the Brewer-Dobson circulation is one of the most robust and consistently projected general-circulation changes to emerge from stratosphere-resolving climate models (Butchart, 2014). In the absence of any other changes affecting the QBO, this would imply a slowing of the QBO (i.e., longer periods) in the models. Such a slowing was reported by Kawatani et al. (2011) and Watanabe and Kawatani (2012) based on single-model projections (Note Giorgetta and Doege (2005) found a shortening of the periods under climate change though their model was unusual in that tropical up-welling decreased), but subsequent analysis of multimodel projections by Kawatani and Hamilton (2013) and Richter, Butchart, et al. (2020) failed to establish a consensus on how the period of the QBO responds to climate change. Somewhat counterintuitively, the oscillation is projected to speed up in 7 of the 10 CMIP6 models analyzed here. Most likely, this is due to projected changes in climate enhancing the wave driving of the QBO such that this more than compensates for the effects of a faster Brewer-Dobson circulation; though without additional diagnostics for analyzing the QBO's momentum budget, it is not possible to confirm this. An approximate balance between competing effects (e.g., enhanced wave driving and a faster Brewer-Dobson circulation) suggests that trends in the QBO period are likely to be small and difficult to detect due to the large cycle-to-cycle variability that is reproduced by the 10 CMIP6 models. This would explain why there is currently no consensus among models on how the QBO period will respond to a changing climate.

Unlike the period response, the QBO amplitude response to climate change appears robust with models consistently projecting a weakening of the oscillation (e.g., Kawatani & Hamilton, 2013; Kawatani et al., 2011; Richter, Butchart, et al., 2020). Results presented above for the SSP370 and SSP585 scenarios, and also the most recent 50 years of the historical simulations, further support the robustness of model projections. Kawatani and Hamilton (2013) argued persuasively that the weakening of the QBO results from an acceleration of the Brewer-Dobson circulation in the models, at least in the lower stratosphere. Higher up, at 20 hPa, the results from the CMIP6 models indicate that decreasing westward amplitudes contribute, on average, roughly 65% of the weakening of the QBO. This is consistent with results of Richter, Butchart, et al. (2020), who noted that when CO_2 amounts were first doubled then quadrupled in idealized experiments, there was no change, on average, in eastward amplitudes at 10 hPa but a systematic decline in westward amplitudes (see Figure 8 in Richter, Butchart, et al., 2020). The reasons for the asymmetric phase response are unclear. Possibly, it is simply a manifestation of common model deficiencies as, for example, models generally represent (e.g., Holt et al., 2020) eastward wave forcing (e.g., Kelvin waves) better than westward wave forcing (e.g., mixed Rossby-gravity waves) and, in turn, stimulated QBOs can be quite sensitive to the ratio of parameterized to resolved forcing in opposite QBO phases. Also, in many models only the resolved waves respond fully to climate change as the parameterized waves typically have fixed sources. However, without additional wave forcing diagnostics, it is not possible to establish whether the asymmetric response seen in the CMIP6 climate projections is due to model deficiencies or genuine physical processes or combination of both.

The projections of how the QBO will respond to climate change have been extended here to include the corresponding oscillation in the equatorial temperatures. As with the QBO in the winds, the QBO in the temperatures weaken in the CMIP6 climate projections, but only above 30 hPa. Largely, this is simply a consequence of the temperatures in the tropics adjusting to perturbations in the winds (e.g., the QBO) to maintain thermal wind balance. Temperature also responds to perturbations in diabatic processes, and below 30 hPa it is possible that the QBO no longer dominates the variability in the temperatures as it did for the zonal winds and, therefore , its amplitude cannot be accurately estimated using the simple Dunkerton and Delisi (1985) approach. Nonetheless, the root mean squares multiplied by the square root of 2 can still be interpreted as a measure of the temperature variability. The results suggest this will increase, on average,

in the models at 50 hPa due to climate change though the uncertainty is large with some models indicating a decrease.

The aim of this study has been to provide an updated assessment of future changes to the QBO based on the latest state-of-the-art climate projections, with the focus on the multimodel mean trends. This has established a weakening of the QBO as one of the more robust dynamical changes occurring in the CMIP6 climate projections. However, more research will be needed, before a weaker QBO can be considered as a potential "fingerprint" of climate change. Models display a wide spread in behavior when simulating the QBO (e.g., see Figures 1 and 2) while also having common deficiencies such as the under representation of QBO amplitudes below 20 hPa (Richter, Anstey, et al., 2020a). In a comprehensive evaluation of our current capabilities for modeling the QBO, Bushell et al. (2020) concluded that there is "work to be done" improving many aspects of the simulated QBOs. Increased confidence in the projected changes to the QBO will also depend on a more in depth analysis of the processes driving the changes than was possible here.

Acknowledgments
This research was supported by the Met Office Hadley Centre Programme funded by BEIS and Defra. N. B. received additional support from UK China Research and Innovation Partnership Fund through the Met Office Climate Science for Service Partnership (CSSP) China as part of the Newton Fund. Y. K. was supported by JSPS KAKENHI Grants JP15KK0178, JP17K18816, and JP18H01286 and by the Environment Research and Technology Development Fund (2-1904) of the Environmental Restoration and Conservation Agency of Japan. J. R. was supported by the National Center for Atmospheric Research, which is a major facility sponsored by the National Science Foundation under Cooperative Agreement 1852977, with additional support from the Regional and Global Model Analysis (RGMA) component of the Earth and Environmental System Modeling Program of the U.S. Department of Energy's Office of Biological and Environmental Research (BER) via the National Science Foundation IA1844590. S. O. was supported by the UK National Centre for Atmospheric Science and the Natural Environment Research Council (NE/N018001/1 and NE/P006779/1). The scientific guidance of the World Climate Research Programme (WCRP) under the framework of the Stratosphere-troposphere Processes and their Role in Climate (SPARC) QBO-initiative (QBOi) is grateful acknowledged for helping to motivate this work. Constructive comments from two anonymous reviewers were also rather useful. Model data used in this study were obtained from the CMIP6 international archive (https://esgf-index1.ceda.ac.uk/projects/cmip6-ceda/). The FUB wind data was obtained online (from https://www.geo.fu-berlin.de/en/met/ag/strat/produkte/qbo).

References

Andrews, D. G., Holton, J. R., & Leovy, C. B. (1987). *Middle atmosphere dynamics*. New York: Academic Press.

Andrews, M. B., Knight, J. R., Scaife, A. A., Lu, Y., Wu, T., Gray, L. J., & Schenzinger, V. (2019). Observed and simulated teleconnections between the stratospheric quasi-biennial oscillation and Northern Hemisphere winter atmospheric circulation. *Journal of Geophysical Research: Atmospheres*, *124*, 1219–1232. https://doi.org/10.1029/2018JD029368

Anstey, J. A., & Shepherd, T. G. (2014). High-latitude influence of the quasi-biennial oscillation. *Quarterly Journal of the Royal Meteorological Society*, *140*(678), 1–21. https://doi.org/10.1002/qj.2132

Balaji, V., Taylor, K. E., Juckes, M., Lawrence, B. N., Durack, P. J., Lautenschlager, M., et al. (2018). Requirements for a global data infrastructure in support of CMIP6. *Geoscientific Model Development*, *11*(9), 3659–3680. https://doi.org/10.5194/gmd-11-3659-2018

Baldwin, M. P., Gray, L. J., Dunkerton, T. J., Hamilton, K., Haynes, P. H., Randel, W. J., et al. (2001). The quasi-biennial oscillation. *Reviews of Geophysics*, *39*(2), 179–229. https://doi.org/10.1029/1999RG000073

Bushell, A. C., Anstey, J. A., Butchart, N., Kawatani, Y., Osprey, S. M., Richter, J. H., et al. (2020). Evaluation of the quasi-biennial oscillation in global climate models for the SPARC QBO-initiative. *Quarterly Journal of the Royal Meteorological Society*. https://doi.org/10.1002/qj.3765

Butchart, N. (2014). The Brewer-Dobson circulation. *Reviews of Geophysics*, *52*, 157–184. https://doi.org/10.1002/2013RG000448

Butchart, N., Anstey, J. A., Hamilton, K., Osprey, S., McLandress, C., Bushell, A. C., et al. (2018). Overview of experiment design and comparison of models participating in phase 1 of the SPARC Quasi-Biennial Oscillation initiative (QBOi). *Geoscientific Model Development*, *11*(3), 1009–1032. https://doi.org/10.5194/gmd-11-1009-2018

Coy, L., Wargan, K., Molod, A. M., McCarty, W. R., & Pawson, S. (2016). Structure and dynamics of the quasi-biennial oscillation in MERRA-2. *Journal of Climate*, *29*(14), 5339–5354. https://doi.org/10.1175/JCLI-D-15-0809.1

Dunkerton, T. J. (1997). The role of gravity waves in the quasi-biennial oscillation. *Journal of Geophysical Research*, *102*, 26,053–26,076. https://doi.org/10.1029/96JD02999

Dunkerton, T. J., & Delisi, D. P. (1985). Climatology of the equatorial lower stratosphere. *Journal of the Atmospheric Sciences*, *42*(4), 376–396. https://doi.org/10.1175/1520-0469(1985)042h0376:COTELSi2.0.CO;2

Ebdon, R. A., & Veryard, R. G. (1961). Fluctuations in equatorial stratospheric winds. *Nature*, *189*, 791–793. https://doi.org/10.1038/189791a0

Eyring, V., Bony, S., Meehl, G. A., Senior, C. A., Stevens, B., Stouffer, R. J., & Taylor, K. E. (2016). Overview of the Coupled Model Intercomparison Project Phase 6 (CMIP6) experimental design and organization. *Geoscientific Model Development*, *9*(5), 1937–1958. https://doi.org/10.5194/gmd-9-1937-2016

Gidden, M. J., Riahi, K., Smith, S. J., Fujimori, S., Luderer, G., Kriegler, E., et al. (2019). Global emissions pathways under different socioeconomic scenarios for use in CMIP6: A dataset of harmonized emissions trajectories through the end of the century. *Geoscientific Model Development*, *12*(4), 1443–1475. https://doi.org/10.5194/gmd-12-1443-2019

Giorgetta, M. A., & Doege, M. C. (2005). Sensitivity of the quasi-biennial oscillation to CO_2 doubling. *Geophysical Research Letters*, *32*, L08701. https://doi.org/10.1029/2004GL021971

Hendon, H. H., & Abhik, S. (2018). Differences in vertical structure of the Madden-Julian oscillation associated with the quasi-biennial oscillation. *Geophysical Research Letters*, *45*, 4419–4428. https://doi.org/10.1029/2018GL077207

Holt, L., Lott, F., Garcia, R. R., Kiladis, G. N., Anstey, J., Braesicke, P., et al. (2020). An evaluation of tropical waves and wave forcing of the QBO in the QBOi models. *Quarterly Journal of the Royal Meteorological Society*, *145*. https://doi.org/10.1002/qj.xxx

IPCC (2013). Climate Change 2013: The Physical Science Basis. Contribution of Working Group I to the Fifth Assessment Report of the Intergovernmental Panel on Climate Change. In S. F. Stocker et al. (Eds.), (pp. 1535). Cambridge, United Kingdom and New York, NY, USA: Cambridge University Press.

Kawatani, Y., & Hamilton, K. (2013). Weakened stratospheric quasi-biennial oscillation driven by increased tropical mean upwelling. *Nature*, *497*, 478–481. https://doi.org/10.1038/nature12140

Kawatani, Y., Hamilton, K., & Watanabe, S. (2011). The quasi-biennial oscillation in a double CO_2 climate. *Journal of the Atmospheric Sciences*, *68*(2), 265–283. https://doi.org/10.1175/2010JAS3623.1

Meinshausen, M., Nicholls, Z., Lewis, J. C., Gidden, M. J., Vogel, E., Freund, M. B., Beyerle, U., Gessner, C., Nauels, A., Bauer, N., Canadell, J. G., Daniel, J. S., John, A., Krummel, P. B., Luderer, G., Meinshausen, N., Montzka, S. A., Rayner, P., Reimann, S., Smith, S. J., Berg, M. V., Velders, G. J., Vollmer, M. K., & Wang, H. J. (2019). *The SSP greenhouse gas concentrations and their extensions to 2500*. https://doi.org/10.5194/gmd-2019-222

Naujokat, B. (1986). An update of the observed quasi-biennial oscillation of the stratospheric winds over the tropics. *Journal of the Atmospheric Sciences*, *43*(17), 1873–1877. https://doi.org/10.1175/1520-0469(1986)043h1873:AUOTOQi2.0.CO;2

O'Neill, B. C., Tebaldi, C., van Vuuren, D. P., Eyring, V., Friedlingstein, P., Hurtt, G., et al. (2016). The Scenario Model Intercomparison Project (ScenarioMIP) for CMIP6. *Geoscientific Model Development*, *9*(9), 3461–3482. https://doi.org/10.5194/gmd-9-3461-2016

Richter, J. H., Anstey, J., Butchart, N., Kawatani, Y., Meehl, G. A., Osprey, S. M., & Simpson, I. R. (2020a). Progress in simulating the quasi-biennial oscillation in CMIP models. *Journal of Geophysical Research: Atmospheres*, *125*, e2019JD032362. https://doi.org/10.1029/2019JD032362

Richter, J. H., Butchart, N., Kawatani, Y., Bushell, A. C., Holt, L., Serva, F., et al. (2020). Response of the quasi-biennial oscillation to a warming climate in global climate models. *Quarterly Journal of the Royal Meteorological Society*. https://doi.org/10.1002/qj.3749

Santer, B. D., Thorne, P. W., Haimberger, L., Taylor, K. E., Wigley, T. M. L., Lanzante, J. R., et al. (2008). Consistency of modelled and observed temperature trends in the tropical troposphere. *International Journal of Climatology*, *28*(13), 1703–1722. https://doi.org/10.1002/joc.1756

Schenzinger, V., Osprey, S., Gray, L., & Butchart, N. (2017). Defining metrics of the quasi-biennial oscillation in global climate models. *Geoscientific Model Development*, *10*(6), 2157–2168. https://doi.org/10.5194/gmd-10-2157-2017

Watanabe, S., & Kawatani, Y. (2012). Sensitivity of the QBO to mean tropical upwelling under a changing climate simulated with an earth system model. *Journal of the Meteorological Society of Japan. Ser. II*, *90A*, 351–360. https://doi.org/10.2151/jmsj.2012-A20